Supporting Information for

Proton Availability at the Air/Water Interface

Shinichi Enami, Michael R. Hoffmann, Agustín J. Colussi*

W. M. Keck Laboratories, California Institute of Technology, California 91125, USA

jz-2010-00322w-R2

EXPERIMENTAL METHODS

Our experiments involve the generation of aqueous microjets in the spraying chamber of an electrospray ionization mass spectrometer (ESI-MS) that is simultaneously flushed with TMA(g)/N_2(g) mixtures at 1 atm, 293 K[1,2] (Fig. S1). $TMAH^+$ ions already present on the surface of the water microjets by acidifying $TMAH^+Cl^-$, or those produced *in situ* during brief exposure to TMA(g), are detected and quantified by online ESI-MS within 1 ms. Solutions pumped through a grounded stainless steel needle, which is coaxial with a sheath issuing nebulizer N_2 gas, surge as a microjet into the chamber.[3] The fast nebulizer gas ($v_g \sim 2.5 \times 10^4$ cm s^{-1}) rapidly shreds the interfacial layers of the slower liquid microjet ($v_j \sim 10$ cm s^{-1}) into charged microjets that carry anion or cation excesses following to a normal probability distribution function.[4,5] On average, the nebulizer gas shreds a 1 μm radius droplet from interfacial liquid layers $\delta \leq 1$ nm thick in a few microseconds. Microjets subsequently lose mass, but retain their excess charges *ze*, via solvent evaporation in the dry, warm N_2(g) emanating from the electrically polarized inlet to the mass spectrometer. Hence, microjets will be drawn to the inlet with increasing acceleration: $a = (ze/m)\ E$. The strong direct correlation between residence time and droplet size ensures that most reactive events occur in TMA(g) collisions with the liquid microjets and nascent microdroplets. The degree of (the relatively slow $k_d = K_A\ k_b \sim 10^{-9.8}$ M $\times\ 10^{10}$ M^{-1} $s^{-1} \sim 1$ s^{-1}) $TMAH^+$ acid dissociation in the microjets is therefore preserved prior to detection ~ 1 ms later.[6] The ESI-MS signals

generated by our instrument are linear transfer functions of the composition of the interfacial layers of the liquid microjet.[7] The inference is that the cationic excess carried by the positively charged nascent microjets and detected by mass spectrometry is proportional to the [cation] in the interfacial layers of the microjet. Similar considerations apply to the titration of $TMAH^+Cl^-$ followed by positive ion ESI-MS (see below). Further experimental details and validation tests may be found in previous publications from our laboratory.[1,2,8]

TMA/N_2 gas mixtures were introduced into the spraying chamber in a direction perpendicular to a stainless steel needle injector and mass spectrometer, respectively. This geometry was chosen to prevent unwanted TMA losses on the wall of the spraying chamber. The TMA concentration in the chamber was calculated from the combined TMA/N_2 mixture and N_2 drying gas flow rates. The [TMA(g)] values reported in the figures throughout correspond to the concentrations actually sensed by microjets in the spraying chamber, which are ~13 times smaller than the values determined from the flow rates due to further dilution by the N_2 drying gas. Gas flows were regulated by calibrated mass flow controllers (MKS) and a needle valve. Typical instrumental parameters were as follows: drying gas flow rate, 13 L min^{-1}; drying gas temperature, 340 ^oC; nebulizer pressure, 2 atm; collector capillary voltage, -3.5 kV; fragmentor voltage, 22 V. TMA gas (1 % or 0.01 % in UHP N_2) was obtained from Matheson-Tri-Gas. D_2O (> 99.9 %) and LiCl (> 99.9 %) were obtained from Sigma-Aldrich. NaCl (> 99.9 %) was obtained from J.T. Baker Chem. Co. H_3PO_4 (85 %) was obtained from Fisher

Scientific. All solutions were prepared in deionized water from a Millipore Milli-Q gradient water purification system. Solution pH_{BLK} was adjusted by adding HCl/NaOH and measured with a calibrated pH meter (VWR). We verified that our solutions did not contain detectable amounts of dissolved atmospheric CO_2 from the absence of HCO_3^- (m/z = 61) via negative ion ESI-MS.

Captions to Figures

Fig. S1 Schematic diagram of the present experimental setup and TMA(g) injection system. MFC stands for mass flow controller.

Fig. S2 Plot of the m/z = 60 signal intensity vs. [TMA·HCl(aq)] in water solution (red circle) and in 100 mM LiCl solution (blue square) at pH_{BLK} ~ 7.

Fig. S3 Positive ion mass spectra of water microjets at various pH_{BLK}'s adjusted with HCl/NaOH and exposed to 1.5 ppmv TMA(g) (A) or 3 ppmv TMA(g) (B, C and D).

Fig. S4. ESI-MS $TMAH^+$ (m/z = 60) signal intensities as functions of pH_{BLK}. Blue downward triangles: water microjets. Yellow upward triangles: 1.5 mM sodium phosphate buffer microjets. Red downward triangles: 15 mM sodium phosphate buffer microjets in experiments under 1 ppmv TMA(g). Signals normalized to $TMAH^+$ = 1 at pH_{BLK} = 1.

Fig. S5. ESI-MS $TMAH^+$ (m/z = 60, blue downward triangles) and $TMALi^+$ (m/z = 66, red upward triangles) signal intensities as functions of log [LiCl] upon exposing LiCl solution microjets at pH_{BLK} 2.9 to 1 ppmv TMA(g).

Fig. S6. ESI-MS $TMAH^+$ (m/z = 60, blue downward triangles) and $TMALi^+$ (m/z = 66, red upward triangles) signal intensities as functions of pH_{BLK} upon exposing 100 mM aqueous LiCl solution microjets to 1 ppmv TMA(g).

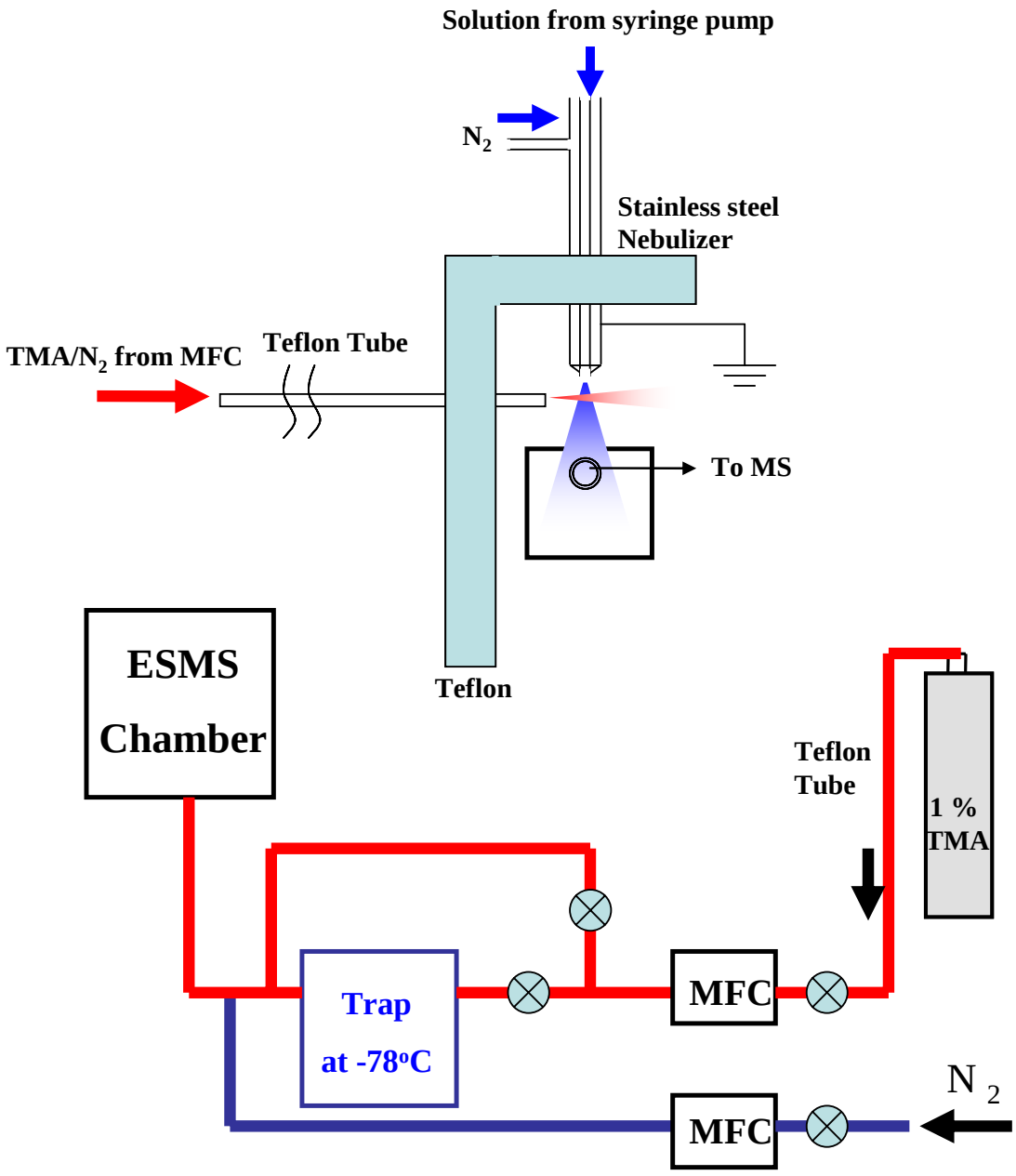
Solution from syringe pump
N2
Stainless steel
Nebulizer
TMA/N2 from MFC
Teflon Tube
To MS
Teflon
ESMS
Chamber
Teflon
Tube
1 %
TMA
Trap
at -78°C
MFC
MFC
N 2

Fig. S1

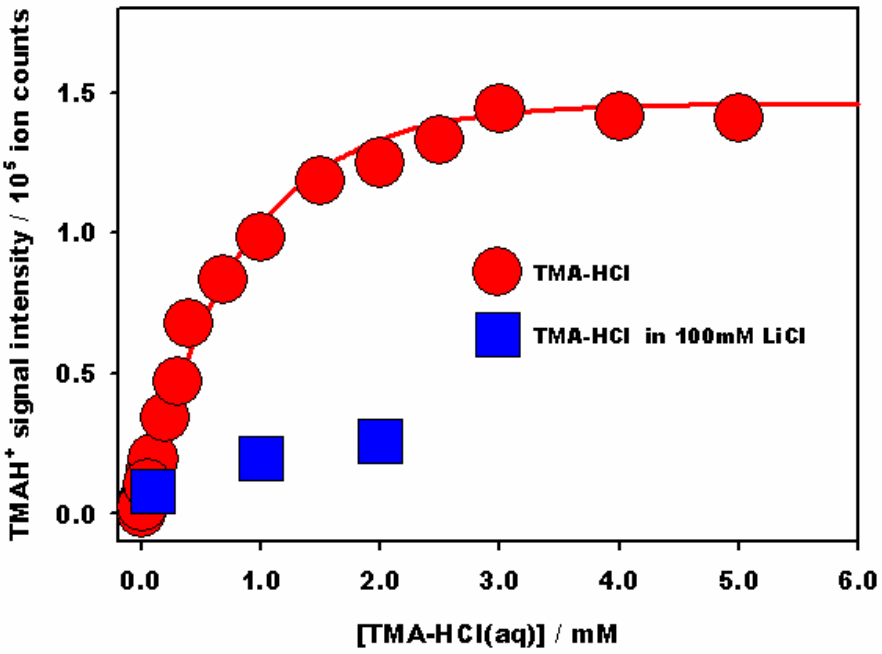
TMAH+ signal intensity / 10^5 ion counts
1.5
1.0
0.5
0.0
0.0
1.0
2.0
3.0
4.0
5.0
6.0
[TMA-HCl(aq)] / mM
TMA-HCl
TMA-HCl in 100mM LiCl

Fig. S2

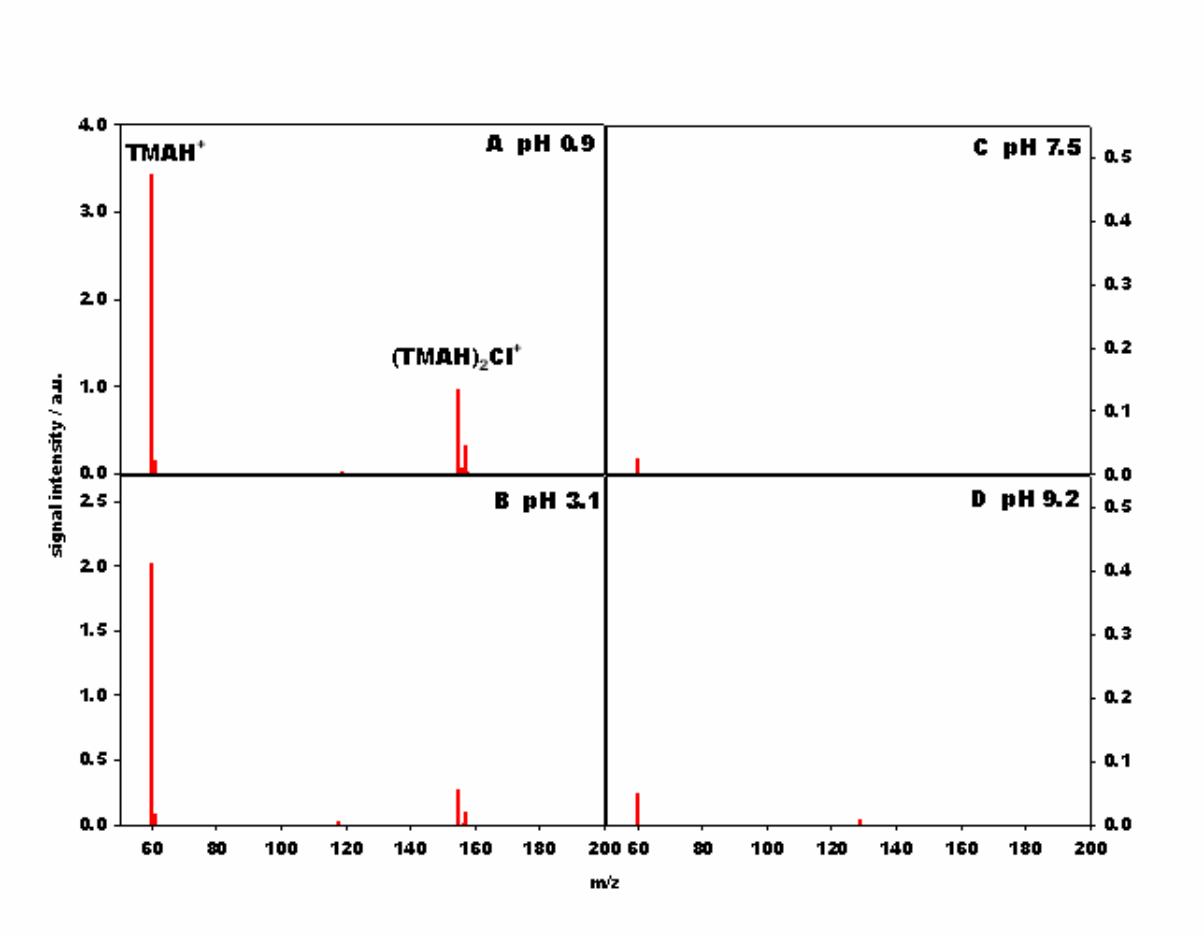
TMAH+
A pH 0.9
(TMAH)2Cl+
C pH 7.5
B pH 3.1
D pH 9.2
signal intensity / a.u.
m/z

Fig. S3

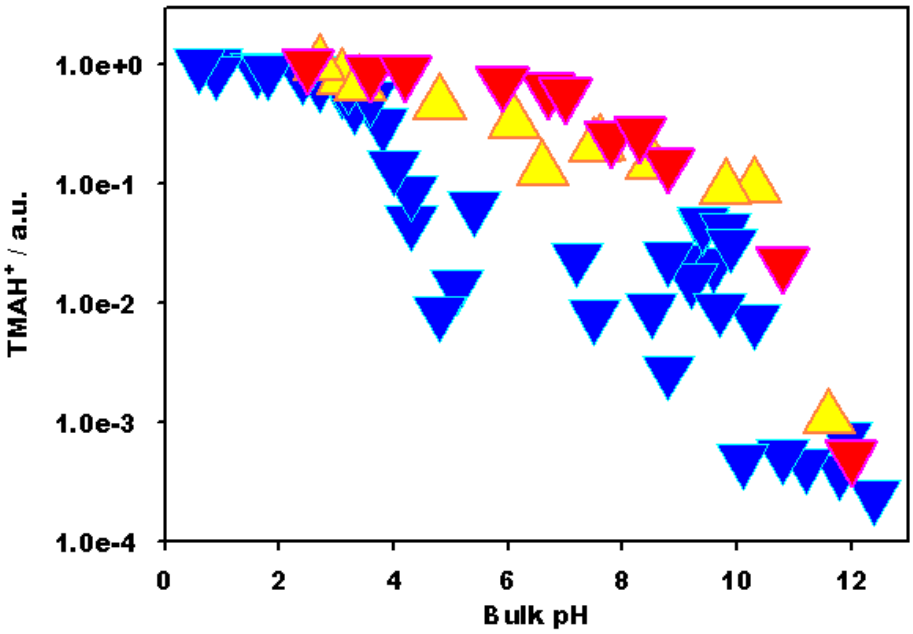

Fig. S4

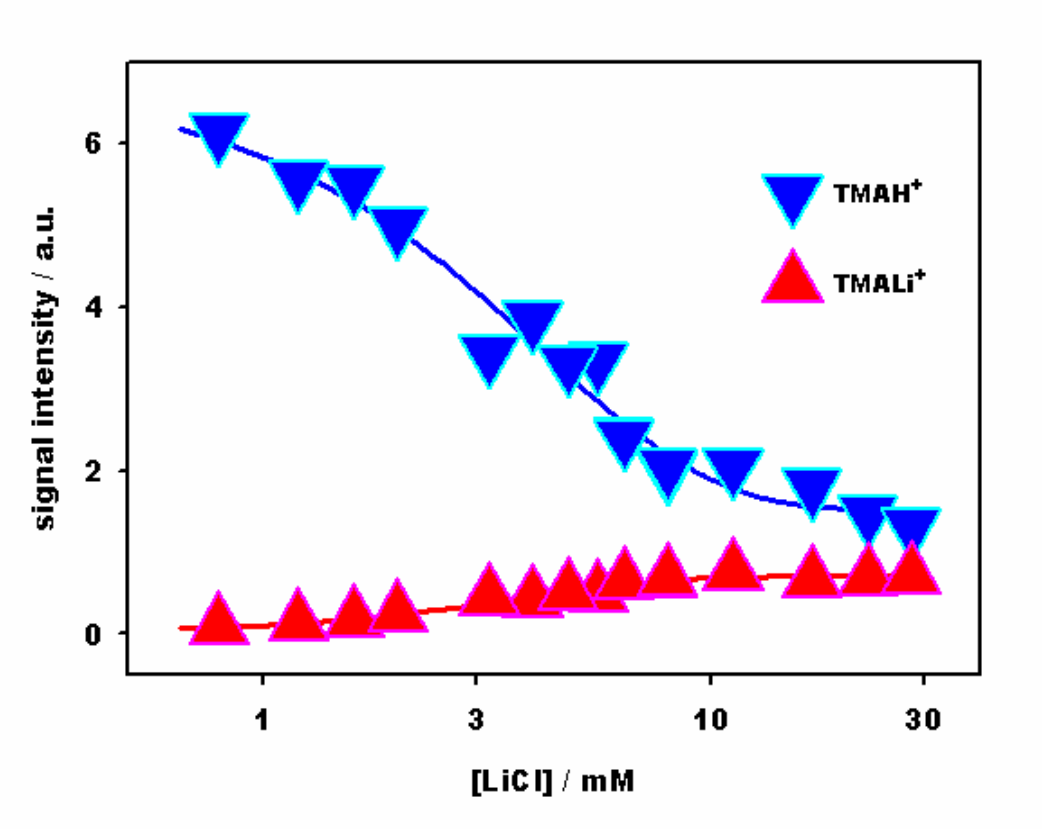

Fig. S5

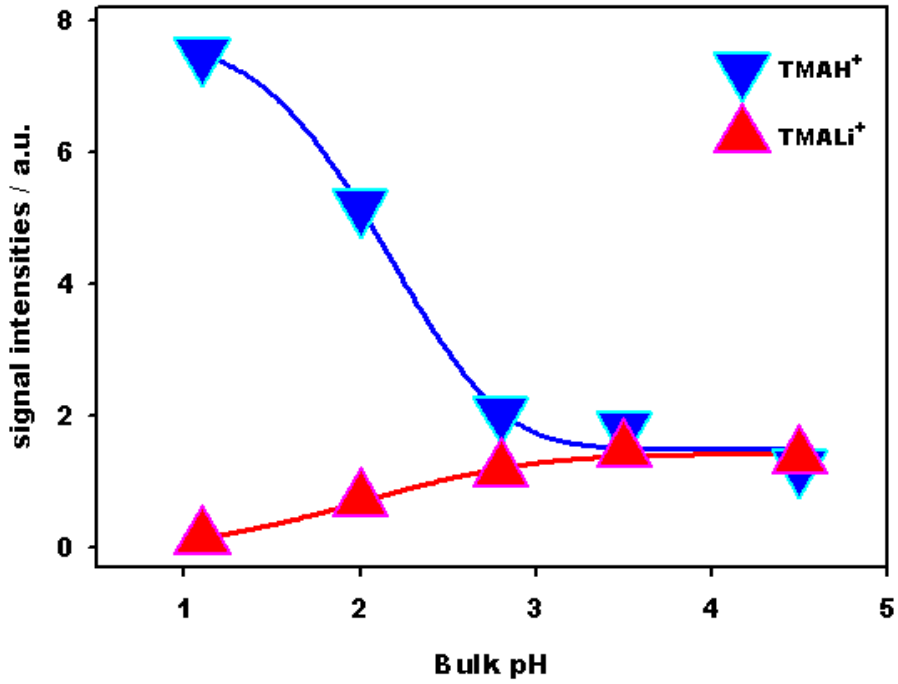

Fig. S6

REFERENCES

(1) Enami, S.; Hoffmann, M. R.; Colussi, A. J. *Proc. Natl. Acad. Sci. U. S. A.* **2008**, *105*, 7365.

(2) Enami, S.; Hoffmann, M. R.; Colussi, A. J. *J. Phys. Chem. A* **2009**, *113*, 7002.

(3) Kebarle, P.; Peschke, M. *Anal. Chim. Acta* **2000**, *406*, 11.

(4) Manisali, I.; Chen, D. D. Y.; Schneider, B. B. *Trends in Analytical Chemistry* **2006**, *25*, 243.

(5) Zilch, L. W.; Maze, J. T.; Smith, J. W.; Ewing, G. E.; Jarrold, M. F. *J. Phys. Chem. A* **2008**, *112*, 13352.

(6) Grunwald, E.; Cocivera, M. *Discuss. Faraday Soc.* **1965**, 105.

(7) Cheng, J.; Psillakis, E.; Hoffmann, M. R.; Colussi, A. J. *J. Phys. Chem. A* **2009**, *113*, 8152.

(8) Enami, S.; Vecitis, C. D.; Cheng, J.; Hoffmann, M. R.; Colussi, A. J. *J. Phys. Chem. A* **2007**, *111*, 13032.